US007757393B2

(12) **United States Patent**
Ayazi et al.

(10) **Patent No.: US 7,757,393 B2**
(45) **Date of Patent: Jul. 20, 2010**

(54) **CAPACITIVE MICROACCELEROMETERS AND FABRICATION METHODS**

(75) Inventors: **Farrokh Ayazi**, Atlanta, GA (US); **Babak Vakili Amini**, Marietta, GA (US); **Reza Abdolvand**, Atlanta, GA (US)

(73) Assignee: **Georgia Tech Research Corporation**, Atlanta, GA (US)

(*) Notice: Subject to any disclaimer, the term of this patent is extended or adjusted under 35 U.S.C. 154(b) by 222 days.

(21) Appl. No.: **11/904,804**

(22) Filed: **Sep. 28, 2007**

(65) **Prior Publication Data**

US 2008/0028857 A1 Feb. 7, 2008

(51) **Int. Cl.**
H05K 3/02 (2006.01)

(52) **U.S. Cl.** **29/847**; 29/25.03; 73/514.01; 73/514.32; 73/514.36; 73/514.38; 73/514.15; 257/301; 257/E27.092; 257/E27.095; 257/E21.651; 257/E29.346; 438/243

(58) **Field of Classification Search** 29/847, 29/25.03; 73/514.01, 514.32, 514.36, 514.38, 73/514.15; 257/301, E27.092, E21.651, 257/E27.095, E29.346; 438/243
See application file for complete search history.

(56) **References Cited**

U.S. PATENT DOCUMENTS

4,414,848 A 11/1983 Shutt
4,719,538 A 1/1988 Cox
4,789,803 A 12/1988 Jacobsen et al.
4,836,034 A 6/1989 Izumi et al.
4,851,080 A 7/1989 Howe et al.
4,882,933 A 11/1989 Petersen et al.
4,891,985 A 1/1990 Glenn
4,905,523 A 3/1990 Okada
4,941,354 A 7/1990 Russell et al.
4,967,605 A 11/1990 Okada
4,969,366 A 11/1990 Okada
5,014,415 A 5/1991 Okada
5,051,643 A 9/1991 Dworsky et al.
5,060,504 A 10/1991 White et al.
5,092,645 A 3/1992 Okada
5,103,667 A 4/1992 Allen et al.
5,124,879 A 6/1992 Goto

(Continued)

OTHER PUBLICATIONS

Allen, H. V., et al. "Self-Testable Accelerometer Systems," *IEEE IC Sensors*, 1989, pp. 113-115.

(Continued)

Primary Examiner—Derris H Banks
Assistant Examiner—Azm Parvez
(74) *Attorney, Agent, or Firm*—Wolf, Greenfield & Sacks, P.C.

(57) **ABSTRACT**

Disclosed are moveable microstructures comprising in-plane capacitive microaccelerometers, with submicro-gravity resolution (<200 ng/√Hz) and very high sensitivity (>17 pF/g). The microstructures are fabricated in thick (>100 μm) silicon-on-insulator (SOI) substrates or silicon substrates using a two-mask fully-dry release process that provides large seismic mass (>10 milli-g), reduced capacitive gaps, and reduced in-plane stiffness. Fabricated devices may be interfaced to a high resolution switched-capacitor CMOS IC that eliminates the need for area-consuming reference capacitors. The measured sensitivity is 83 mV/mg (17 pF/g) and the output noise floor is −91 dBm/Hz at 10 Hz (corresponding to an acceleration resolution of 170 ng/√Hz). The IC consumes 6 mW power and measures 0.65 mm^2 core area.

9 Claims, 9 Drawing Sheets

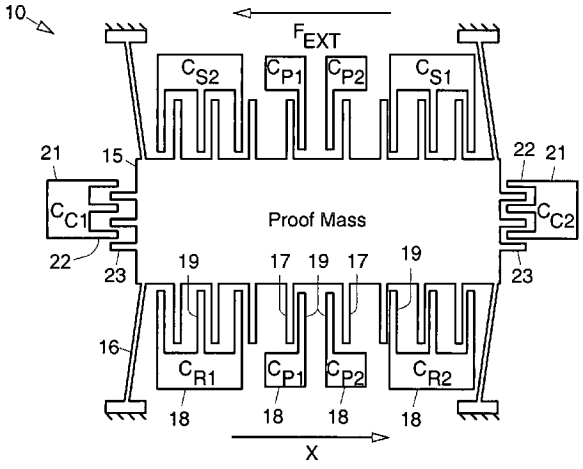

U.S. PATENT DOCUMENTS

5,134,883 A 8/1992 Shannon
5,182,515 A 1/1993 Okada
5,243,861 A 9/1993 Kloeck et al.
5,253,510 A 10/1993 Allen et al.
5,263,375 A 11/1993 Okada
5,295,386 A 3/1994 Okada
5,317,922 A 6/1994 Bomback et al.
5,343,765 A 9/1994 Okada
5,343,766 A 9/1994 Lee et al.
5,392,658 A 2/1995 Okada
5,406,848 A 4/1995 Okada
5,421,213 A 6/1995 Okada
5,428,996 A 7/1995 Abbink et al.
5,437,196 A 8/1995 Okada
5,447,051 A 9/1995 Hanks et al.
5,457,993 A 10/1995 Sapuppo
5,485,749 A 1/1996 Nohara et al.
5,487,305 A 1/1996 Ristic et al.
5,492,020 A 2/1996 Okada
5,497,668 A 3/1996 Okada
5,531,002 A 7/1996 Okada
5,531,092 A 7/1996 Okada
5,567,880 A 10/1996 Yokota et al.
5,571,972 A 11/1996 Okada
5,639,973 A 6/1997 Okada
5,646,346 A 7/1997 Okada
5,661,235 A 8/1997 Bonin
5,675,086 A 10/1997 Kihara et al.
5,682,000 A 10/1997 Okada
5,725,785 A 3/1998 Ishida et al.
5,744,718 A 4/1998 Okada
5,780,749 A 7/1998 Okada
5,786,997 A 7/1998 Hoyt et al.
5,811,693 A 9/1998 Okada
5,831,163 A 11/1998 Okada
5,856,620 A 1/1999 Okada
5,877,421 A 3/1999 Biebl et al.
5,889,242 A 3/1999 Ishihara et al.
5,962,787 A 10/1999 Okada et al.
5,963,788 A 10/1999 Barron et al.
5,987,985 A 11/1999 Okada
6,053,057 A 4/2000 Okada
6,065,341 A 5/2000 Ishio et al.
6,074,890 A * 6/2000 Yao et al. 438/52
6,117,701 A 9/2000 Buchan et al.
6,122,965 A 9/2000 Seidel et al.
6,136,212 A 10/2000 Mastrangelo et al.
6,151,966 A 11/2000 Sakai et al.
6,158,291 A 12/2000 Okada
6,159,761 A 12/2000 Okada
6,166,581 A 12/2000 Liu et al.
6,167,757 B1 * 1/2001 Yazdi et al. 73/514.32
6,169,321 B1 1/2001 Nguyen et al.
6,185,814 B1 2/2001 Okada
6,199,874 B1 * 3/2001 Galvin et al. 280/5.514
6,271,830 B1 8/2001 Berstis
6,276,207 B1 8/2001 Sakai et al.
6,282,956 B1 9/2001 Okada
6,287,885 B1 9/2001 Muto et al.
6,301,965 B1 10/2001 Chu et al.
6,307,298 B1 10/2001 O'Brien
6,314,823 B1 11/2001 Okada
6,344,618 B1 2/2002 Sato
6,378,381 B1 4/2002 Okada et al.
6,386,032 B1 5/2002 Lemkin et al.
6,389,899 B1 5/2002 Partridge et al.
6,401,536 B1 6/2002 O'Brien
6,402,968 B1 6/2002 Yazdi et al.
6,437,772 B1 8/2002 Zimmerman et al.
6,474,133 B1 11/2002 Okada
6,477,903 B2 11/2002 Okada
6,497,149 B1 12/2002 Moreau et al.
6,512,364 B1 1/2003 Okada
6,534,413 B1 3/2003 Robertson et al.
6,581,465 B1 6/2003 Waters et al.
6,596,236 B2 7/2003 DiMeo et al.
6,617,657 B1 9/2003 Yao et al.
6,674,140 B2 1/2004 Martin
6,674,383 B2 1/2004 Horsley et al.
6,683,358 B1 1/2004 Ishida et al.
6,694,814 B2 2/2004 Ishio
6,716,253 B2 4/2004 Okada
6,717,488 B2 4/2004 Potter
6,739,189 B2 5/2004 Lee et al.
6,744,335 B2 6/2004 Ryhanen et al.
6,772,632 B2 8/2004 Okada
6,779,408 B2 8/2004 Okada
6,803,637 B2 10/2004 Benzel et al.
6,841,861 B2 1/2005 Brady
6,864,677 B1 3/2005 Okada
6,865,943 B2 3/2005 Okada
6,894,482 B2 5/2005 Okada
6,897,854 B2 5/2005 Cho et al.
6,743,656 B2 6/2005 Orcutt et al.
6,909,221 B2 6/2005 Ayazi et al.
6,913,941 B2 7/2005 O'Brien et al.
6,920,788 B2 7/2005 Okada
6,925,875 B2 8/2005 Silverbrook
6,936,491 B2 8/2005 Partridge et al.
6,936,492 B2 8/2005 McNeil et al.
6,936,494 B2 8/2005 Cheung
6,938,484 B2 * 9/2005 Najafi et al. 73/514.32
6,941,810 B2 9/2005 Okada
6,469,909 B2 10/2005 Simmons
6,952,041 B2 10/2005 Lutz et al.
6,953,985 B2 10/2005 Lin et al.
6,960,488 B2 11/2005 Brosnihan et al.
7,013,730 B2 3/2006 Malametz
7,023,065 B2 4/2006 Ayazi et al.
7,043,985 B2 5/2006 Ayazi et al.
7,059,188 B2 6/2006 Okada
7,078,796 B2 7/2006 Dunn et al.
7,109,727 B2 9/2006 Hayakawa et al.
7,152,485 B2 12/2006 Okada
7,176,770 B2 2/2007 Ayazi et al.
7,231,802 B2 6/2007 Okada
7,318,349 B2 1/2008 Vaganov et al.
7,337,671 B2 3/2008 Ayazi et al.
7,360,423 B2 4/2008 Ayazi et al.
7,360,455 B2 4/2008 Okada
7,363,814 B2 4/2008 Okada
7,367,232 B2 5/2008 Vaganov et al.
7,543,496 B2 6/2009 Ayazi et al.
2001/0002731 A1 6/2001 Ueda
2001/0011887 A1 8/2001 Sturm et al.
2002/0014126 A1 2/2002 Okada
2002/0020689 A1 2/2002 Leung
2002/0038897 A1 4/2002 Tuan et al.
2002/0040602 A1 4/2002 Okada
2002/0055236 A1 5/2002 Chen
2002/0063322 A1 5/2002 Robbins et al.
2002/0104378 A1 8/2002 Stewart
2002/0117728 A1 8/2002 Brosnihhan et al.
2002/0148534 A2 10/2002 Davis et al.
2003/0122227 A1 7/2003 Silverbrook
2003/0209075 A1 * 11/2003 Okada 73/514.16
2004/0115937 A1 6/2004 Nagai et al.
2004/0187578 A1 9/2004 Malametz et al.
2004/0189340 A1 9/2004 Okada
2004/0231420 A1 11/2004 Xie et al.
2004/0233503 A1 11/2004 Kimura
2004/0245586 A1 12/2004 Partridge et al.
2005/0036269 A1 2/2005 Ma et al.
2005/0095813 A1 5/2005 Zhu et al.

2005/0109108	A1	5/2005	Chen et al.	
2005/0140356	A1	6/2005	Inglese et al.	
2005/0160814	A1	7/2005	Vaganov et al.	
2005/0183503	A1*	8/2005	Malametz	73/514.01
2005/0277218	A1	12/2005	Nakajo et al.	
2005/0287760	A1	12/2005	Yan et al.	
2006/0014374	A1	1/2006	Barth et al.	
2006/0180898	A1	8/2006	Funaki et al.	
2006/0272413	A1	12/2006	Vaganov et al.	
2006/0273416	A1	12/2006	Ayazi et al.	
2007/0012109	A1	1/2007	Okada	
2007/0220971	A1	9/2007	Ayazi et al.	
2007/0256469	A1	11/2007	Okada	
2007/0281381	A1	12/2007	Ayazi	
2008/0028857	A1	2/2008	Ayazi et al.	
2009/0064781	A1	3/2009	Ayazi et al.	
2009/0095079	A1	4/2009	Ayazi	
2009/0266162	A1	10/2009	Ayazi et al.	
2009/0280594	A1	11/2009	Mehregany	

OTHER PUBLICATIONS

Chae, J. et al., "An In-Plane High-Sensitivity, Low-Noise Micro-G Silicon Accelerometer," *Proceedings of MEMS-03 Kyoto, IEEE the Sixteenth Annual International Conference on Micro Electro Mechanical Systems*, 2003, pp. 466-469.

Hao, Z. et al., "A High-Q Length-Extensional Bulk-Mode Mass Sensor with Annexed Sensing Platforms," 4 pages.

Hitachi Metals, Ltd., "Piezoresistive-Type Triaxial Accelerating Sensor," http://hitachimetals.co.jp/e/prod/prod14/p14_03.html, 2 pages.

Jono, K. et al., "Electrostatic servo system for multi-axis accelerometers," *IEEE*, 1994, pp. 251-256.

Jono, K. et al. "An Electrostatic Servo-Type Three-Axis Silicon Accelerometer," *Meas. Sci. Technol.*, 1995, pp. 11-15, vol. 6.

Kulah, H. et al., "A Multi-Step Electromechanical ΣΔ Converter for Micro-g Capacitive Accelerometers," 2003 *IEEE International Solid-State Circuits Conference*, Feb. 11, 2003, 10 pages.

Lemkin, M. A. et al., "A 3-Axis Force Balanced Accelerometer Using a Single Proof-Mass," *Transducers* '97, 1997 *International Conference on Solid-State Sensors and Actuators*, pp. 1185-1188.

Mineta, T. et al., "Three-axis capacitive accelerometer with uniform axial sensitivities," *J. Micromech. Microeng.*, 1996, pp. 431-435, vol. 6.

Mizuno, J. et al., "Silicon Bulk Micromachined Accelerometer with Simultaneous Linear and *Angular Sensitivity," Transducers '97, 1997 International Conference on Solid-State Sensors and Actuators*, pp. 1197-1200.

Monajemi, P. et al., "Thick single crystal silicon MEMS with high aspect ratio vertical air-gaps," *SPIE* 2005 *Micromachining/ Microfabrication Process Technology*, pp. 138-147.

Okada, K., "Tri-Axial Piezoelectric Accelerometer," *Transducers* '95, *The 8th International Conference on Solid-State Sensors and Actuators*, Jun. 25-29, 1995, pp. 566-569.

Pourkamali, S. et al., "High frequency capacitive micromechanical resonators with reduced motional resistance using the HARPSS technology," *Proceedings of 5th Silicon RF topical meeting*, 2004, 4 pages.

Pourkamali, S. et al. "VHF single crystal capacitive elliptic bulk-mode disk resonators —Part II: Implementation and characterization," *Journal of Microelectromechanical Systems*, Dec. 2004, pp. 1054-1062, vol. 13, No. 6.

Pourkamali, S. et al. "Vertical Capacitive SiBARs" *IEEE 2005*, pp. 211-214.

Puers, R. et al., "Design and processing experiments of a new miniaturized capacitive triaxial accelerometer," *Sensors and Actuators A*, 1998, pp. 324-328, vol. 68.

NASA—Space Acceleration Measurement System (SAMS), http://microgravity.grc.nasa.gov/MSD/MSDhtmlslsamsff.html, 4 pages printed Mar. 12, 2010.

Takao, H., et al. "Three Dimensional Vector Accelerometer Using SOI Structure for High Temperature," *Transducers* '95, *The 8th International Conference on Solid-State Sensors and Actuators*, Jun. 25-29, 1995, pp. 683-686.

Vakili Amini, B. et al. "A 2.5 V 14-bit ΣΔ CMOS-SOI capacitive accelerometer," *Proc. IEEE Int. Solid-State Circuits Conf.*, Feb. 18, 2004, 3 pages.

Vakili Amini, B. et al., "A 4.5 mW closed-loop ΔΣ micro-gravity CMOS-SOI accelerometer," *Proc. IEEE Int. Solid-State Circuits Conf.*, Feb. 7, 2006, pp. 288-289, 654.

Vakili Amini, B. et al., "A 4.5 mW closed-loop ΔΣ micro-gravity CMOS-SOI accelerometer," Powerpoint Slide Presentation at *IEEE Int. Solid-State Circuits Conf.*, Feb. 7, 2006, 42 pages.

Vakili Amini, B. et al., "A 4.5 mW closed-loop ΔΣ micro-gravity CMOS-SOI accelerometer," *IEEE Journal of Solid State Circuits*, Dec. 2006, pp. 2983-2991, vol. 41, No. 12.

Vakili Amini, B. et al., "A high resolution, stictionless, CMOS compatible SOI accelerometer with a low noise, low power, 0.25μm CMOS interface," Proc. *IEEE Int. Micro Electro Mechanical Syst. 2004*, pp. 572-575.

Vakili Amini, B. et al., "A new input switching scheme for a capacitive micro-g accelerometer," *Proc. Symposium on VLSI Circuits* 2004, pp. 310-313.

Vakili Amini, B. et al. "Micro-gravity capacitive silicon-on-insulator accelerometers," *Journal of Micromechanics and Microengineering*, Oct. 2005, pp. 2113-2120, vol. 15, No. 11.

Vakili Amini, B. et al., "Sub-micro-gravity capacitive SOI microaccelerometers," *Proc. of the 13th International Conference on Solid State Sensors, Actuators and Microsystems* (*Transducers* '05), pp. 515-518.

Vakili Amini, B., et al., "A. 2.5 V 14-bit ΣΔ CMOS-SOI capacitive accelerometer," *IEEE Journal of Solid-State Circuits*, Dec. 2004, pp. 2467-2476, vol. 39, No. 12.

Watanabe, Y., et al., "Five-axis motion sensor with electrostatic drive and capacitive detection fabricated by silicon bulk micromachining," *Sensors and Actuators A*, 2002, pp. 109-115.

Wu, J. et al., "A Low-Noise Low-Offset Capacitive Sensing Amplifier for a 50-μg/√Hz Monolithic CMOS MEMS Accelerometer," *IEEE Journal of Solid-State Circuits*, May 2004, pp. 722-730, vol. 39, No. 5.

* cited by examiner

Fig. 1

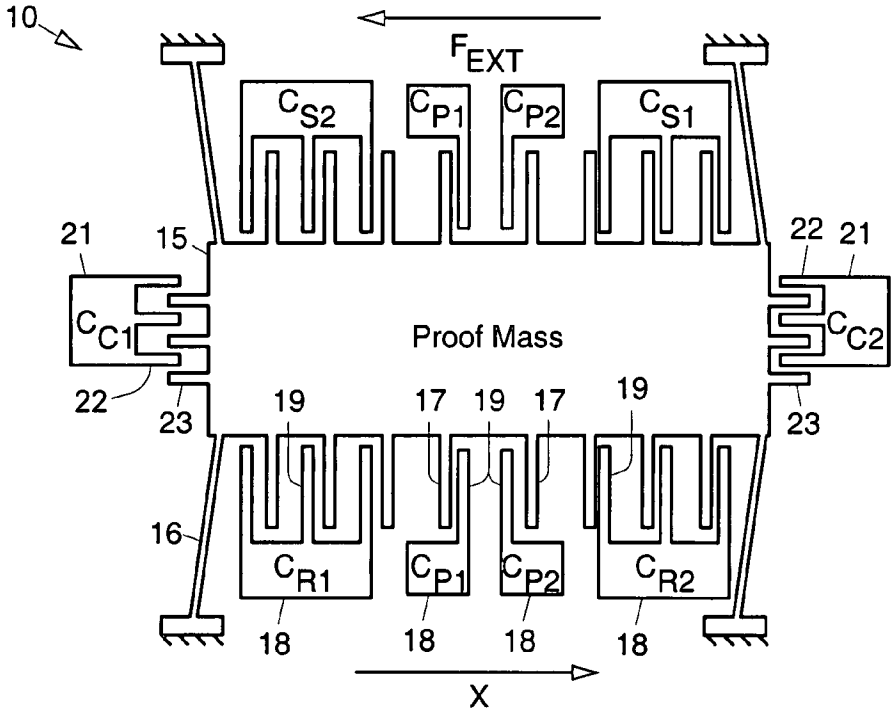
10
F_{EXT}
C_{S2}
C_{P1}
C_{P2}
C_{S1}
21
15
22
21
C_{C1}
Proof Mass
C_{C2}
22
23
19
17
19
17
19
23
16
C_{R1}
C_{P1}
C_{P2}
C_{R2}
18
18
18
18
X

Fig. 2

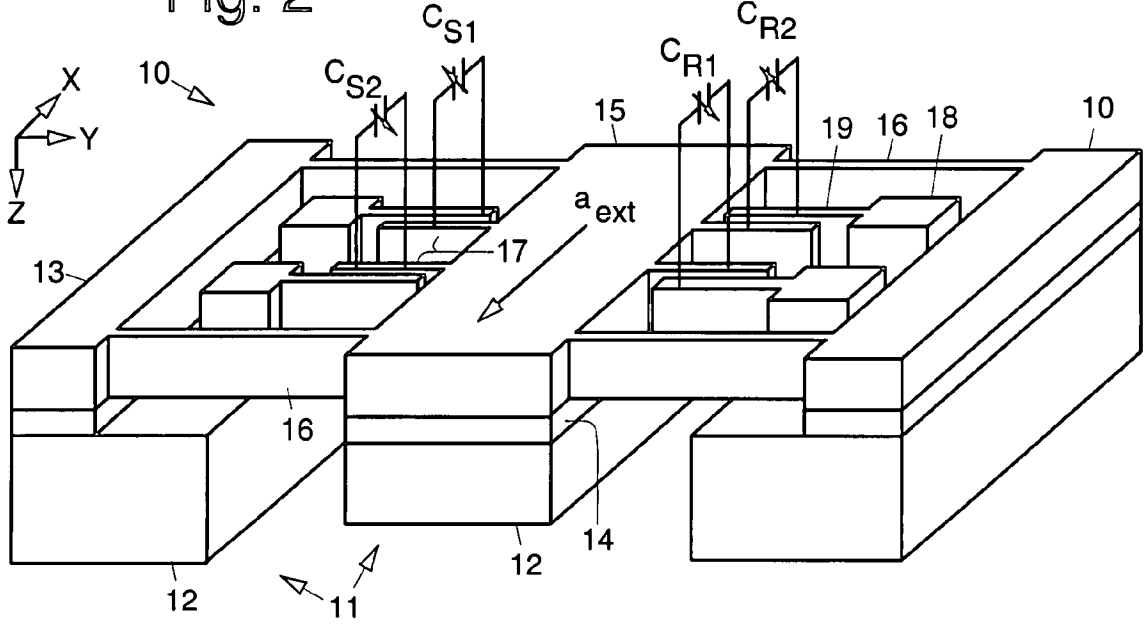
C_{S1}
C_{R2}
C_{R1}
X
10
C_{S2}
Y
Z
15
19
16
18
10
a_{ext}
17
13
16
14
12
12
11

Fig. 3a

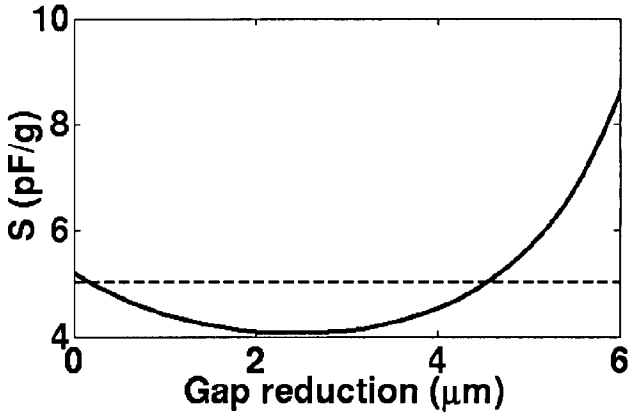

Fig. 3b

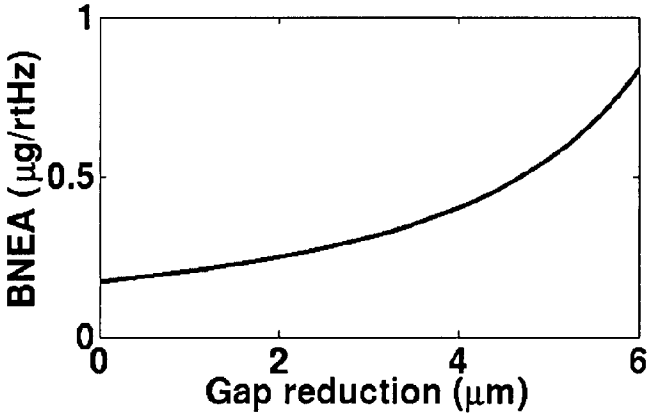

Fig. 3c

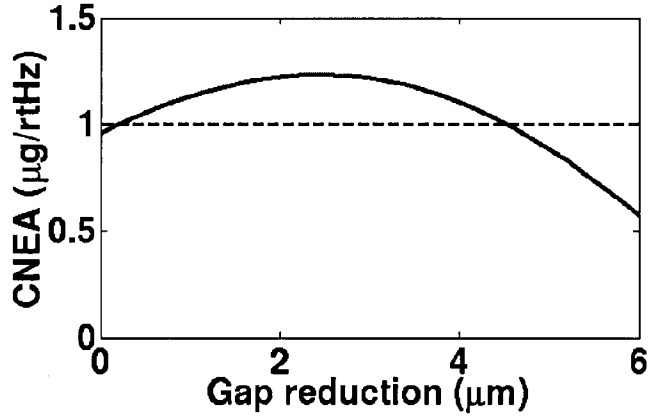

Fig. 3d

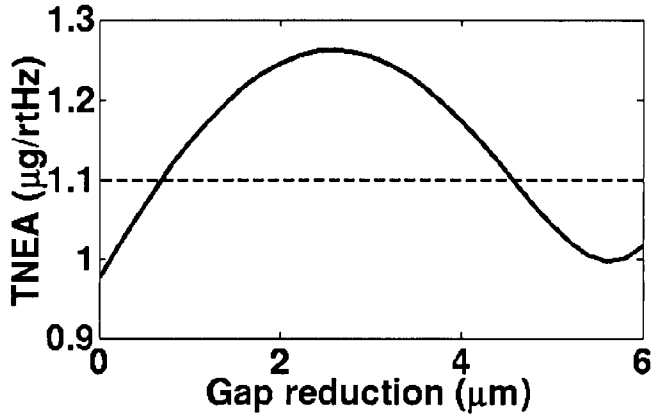

Fig. 3e

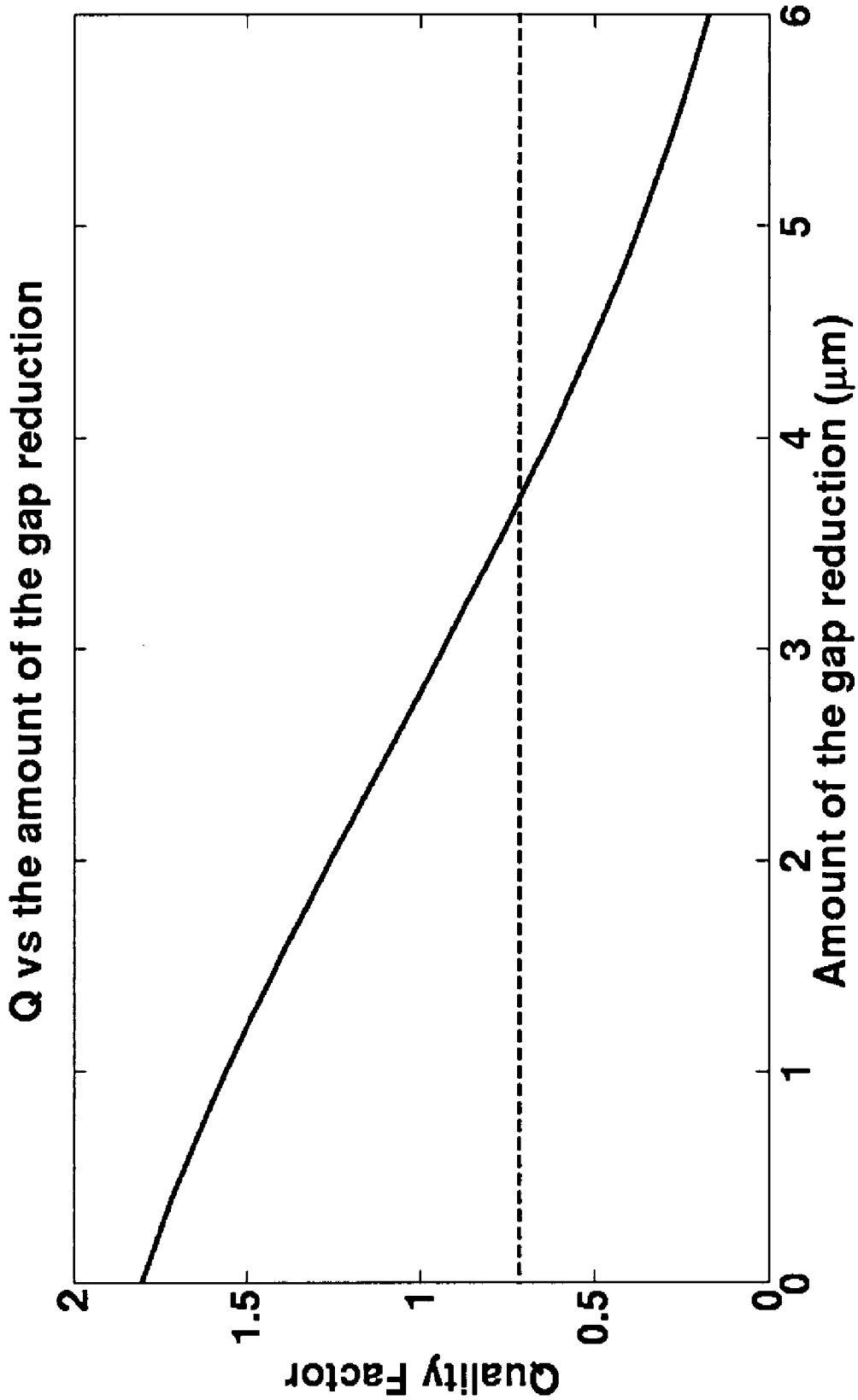
Q vs the amount of the gap reduction
Quality Factor
Amount of the gap reduction (μm)
2
1.5
1
0.5
0
0
1
2
3
4
5
6

Fig. 4a

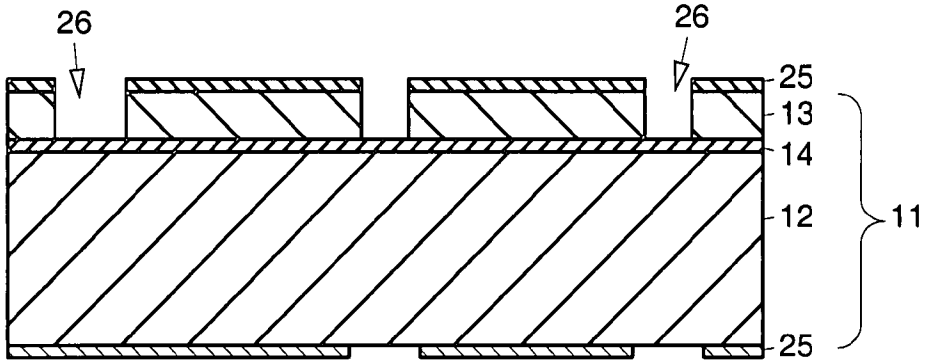

Fig. 4b

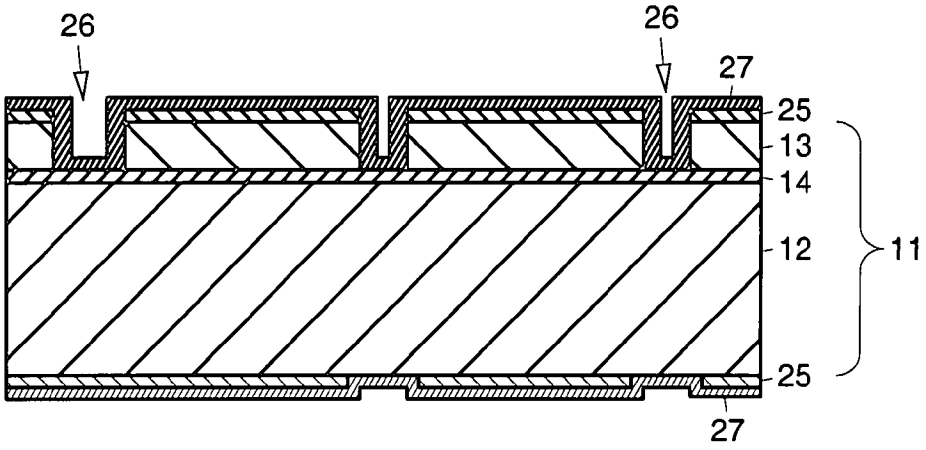

Fig. 4c

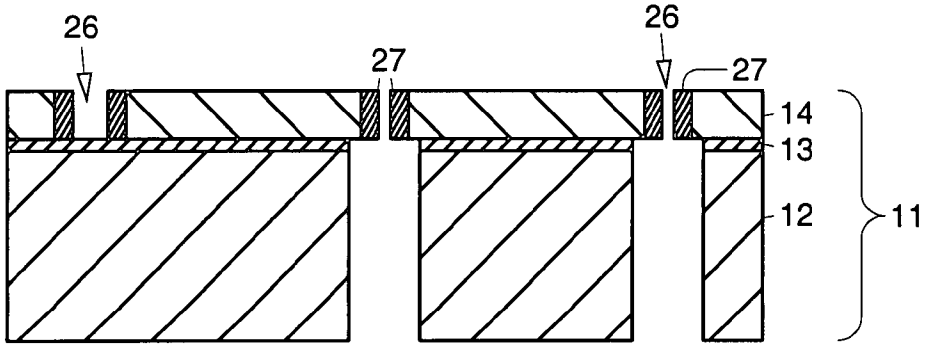

Fig. 4d

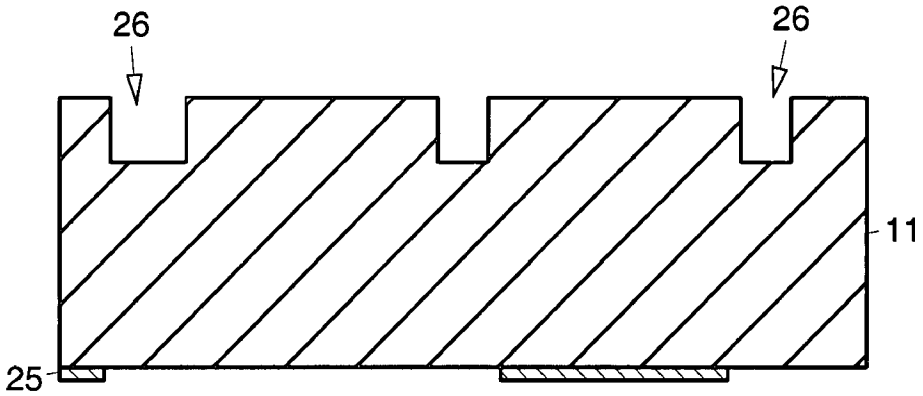

Fig. 4e

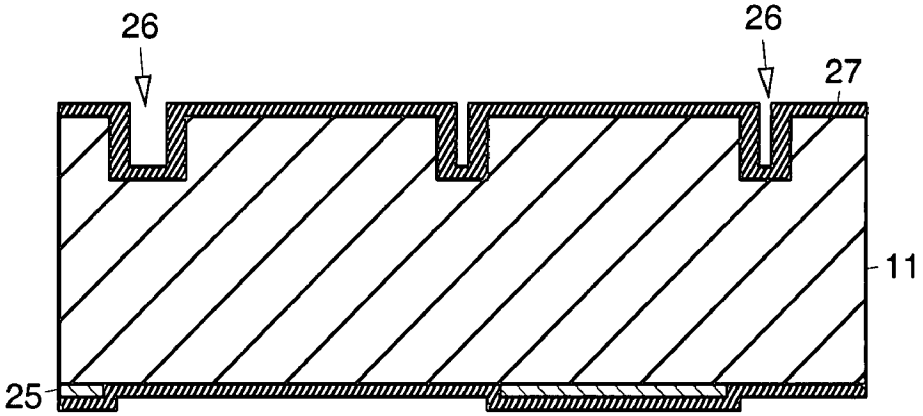

Fig. 4f

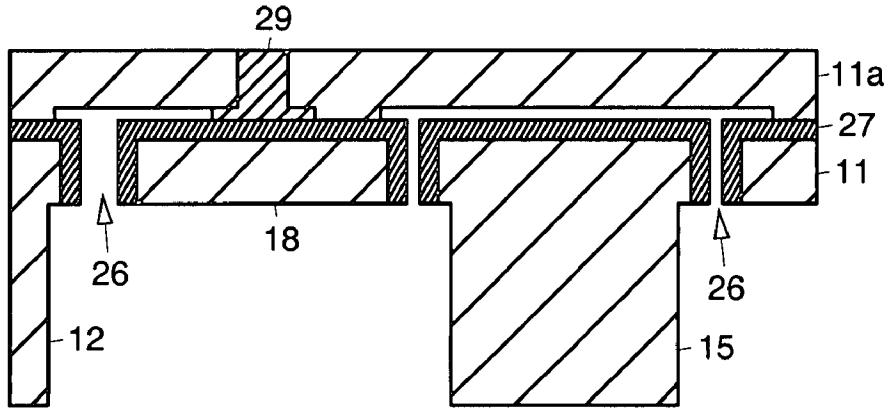

Fig. 5a

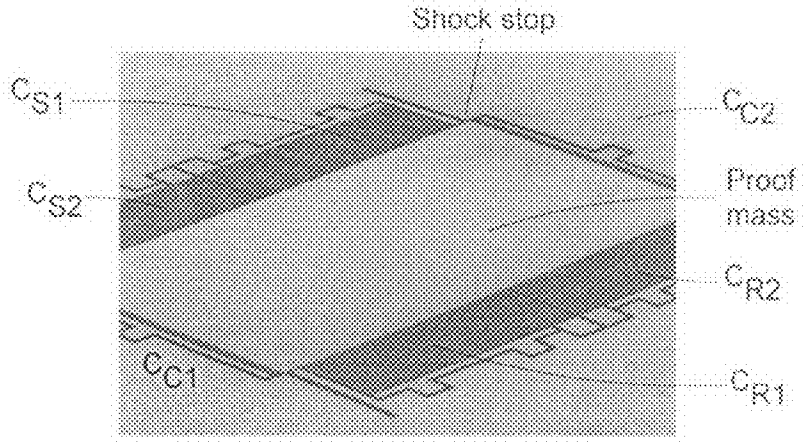

Fig. 5b

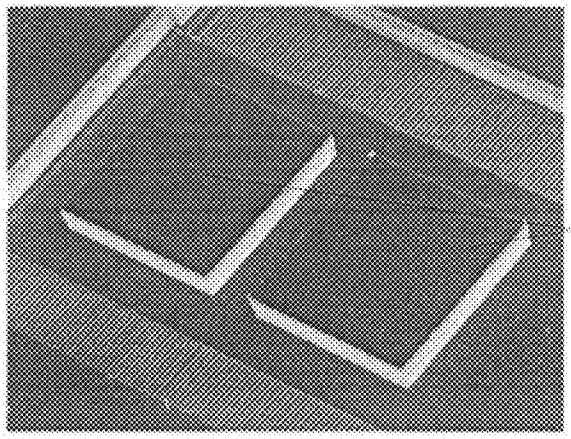

Fig. 5c

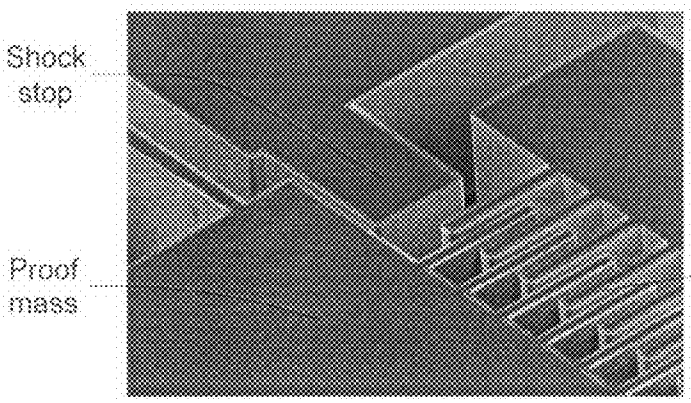

Fig. 5d

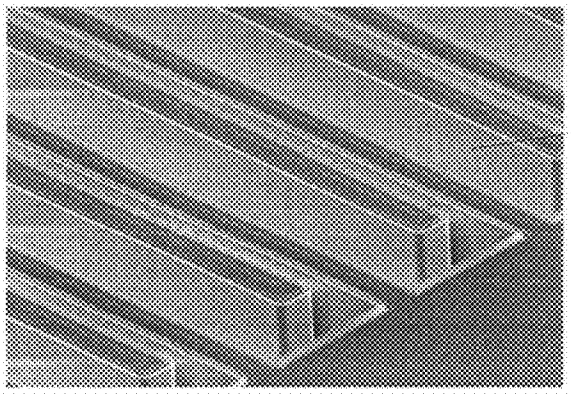

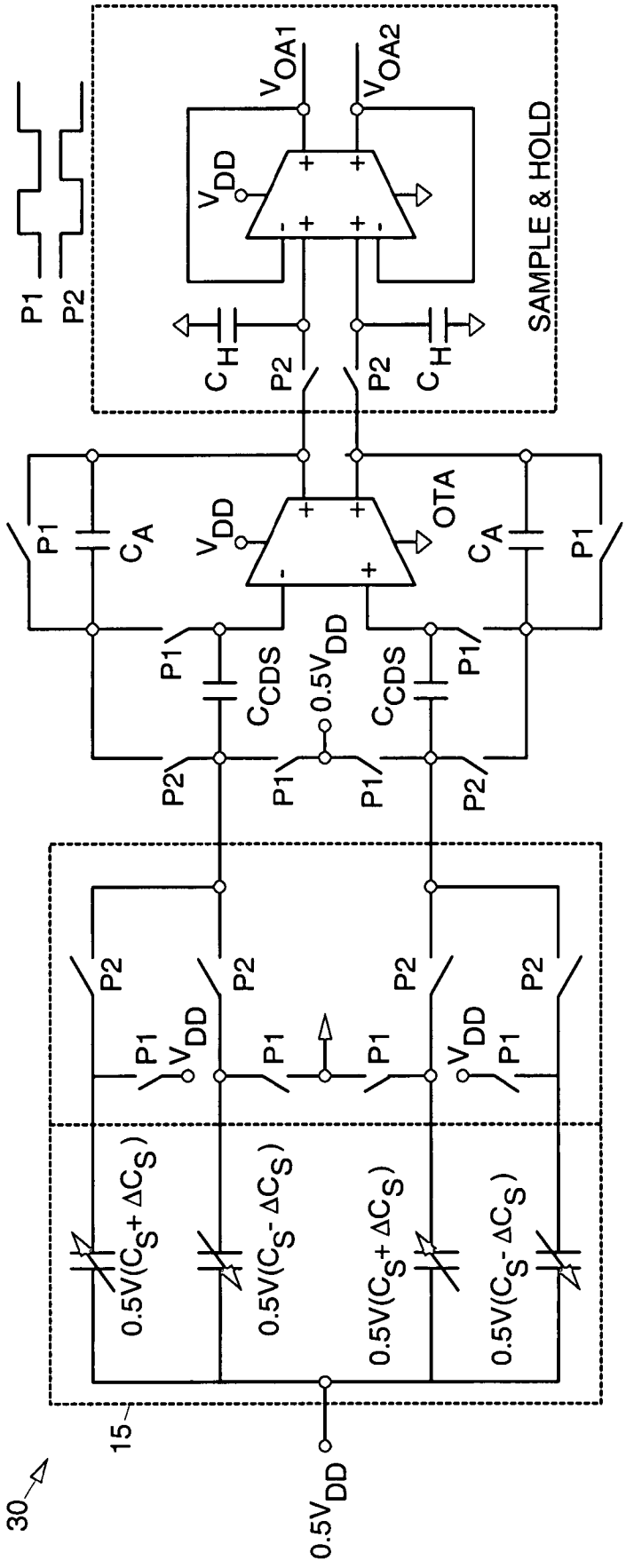
SAMPLE & HOLD
V_{OA1}
V_{OA2}
V_{DD}
P1
P2
C_H
OTA
C_A
C_{CDS}
$0.5V_{DD}$
$0.5V(C_S+\Delta C_S)$
$0.5V(C_S-\Delta C_S)$
15
30

Fig. 6a

Fig. 6b

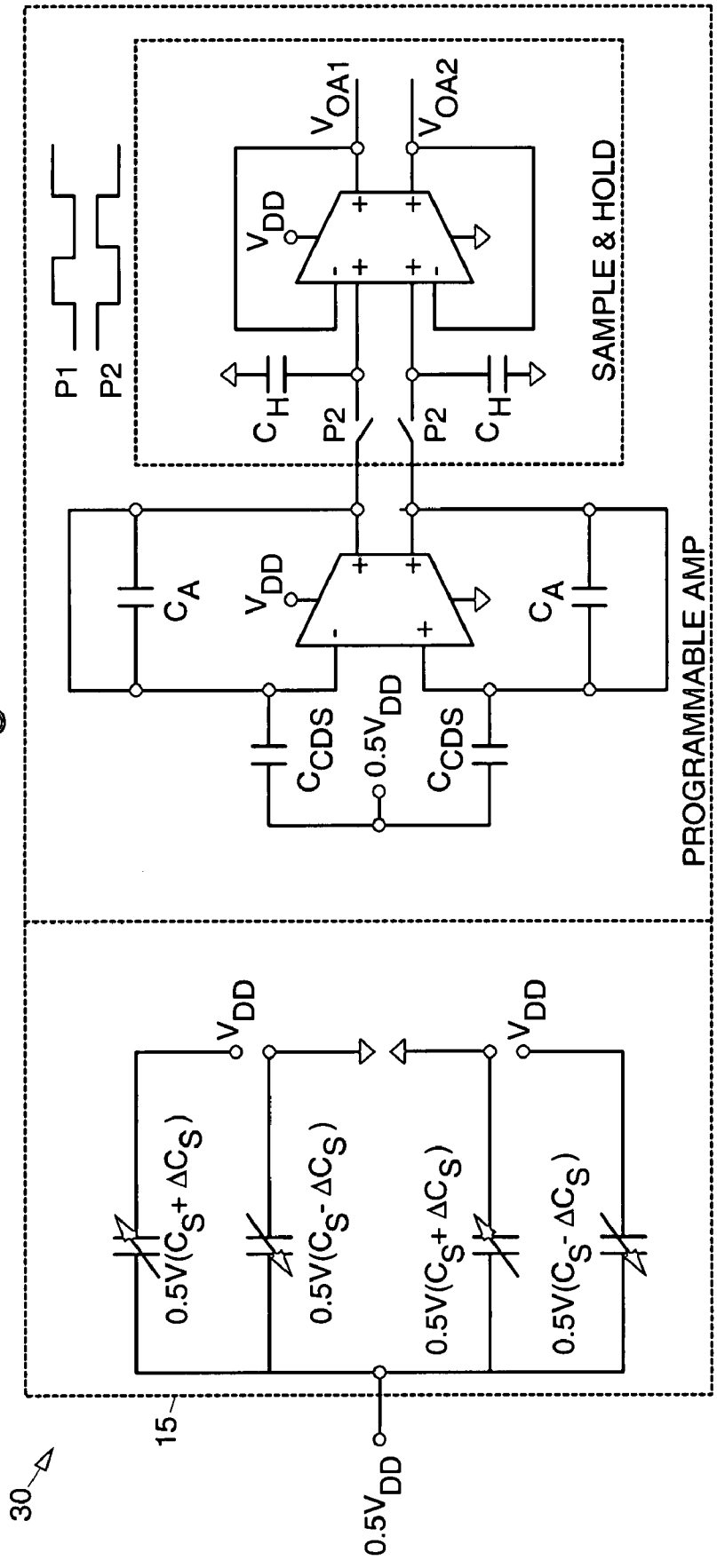
30
15
0.5V_DD
V_DD
0.5V(C_S+ ΔC_S)
0.5V(C_S- ΔC_S)
0.5V(C_S+ ΔC_S)
0.5V(C_S- ΔC_S)
V_DD
V_DD
PROGRAMMABLE AMP
C_CDS
0.5V_DD
C_CDS
C_A
V_DD
C_A
SAMPLE & HOLD
V_OA1
V_OA2
V_DD
C_H
P2
P2
C_H
P1
P2

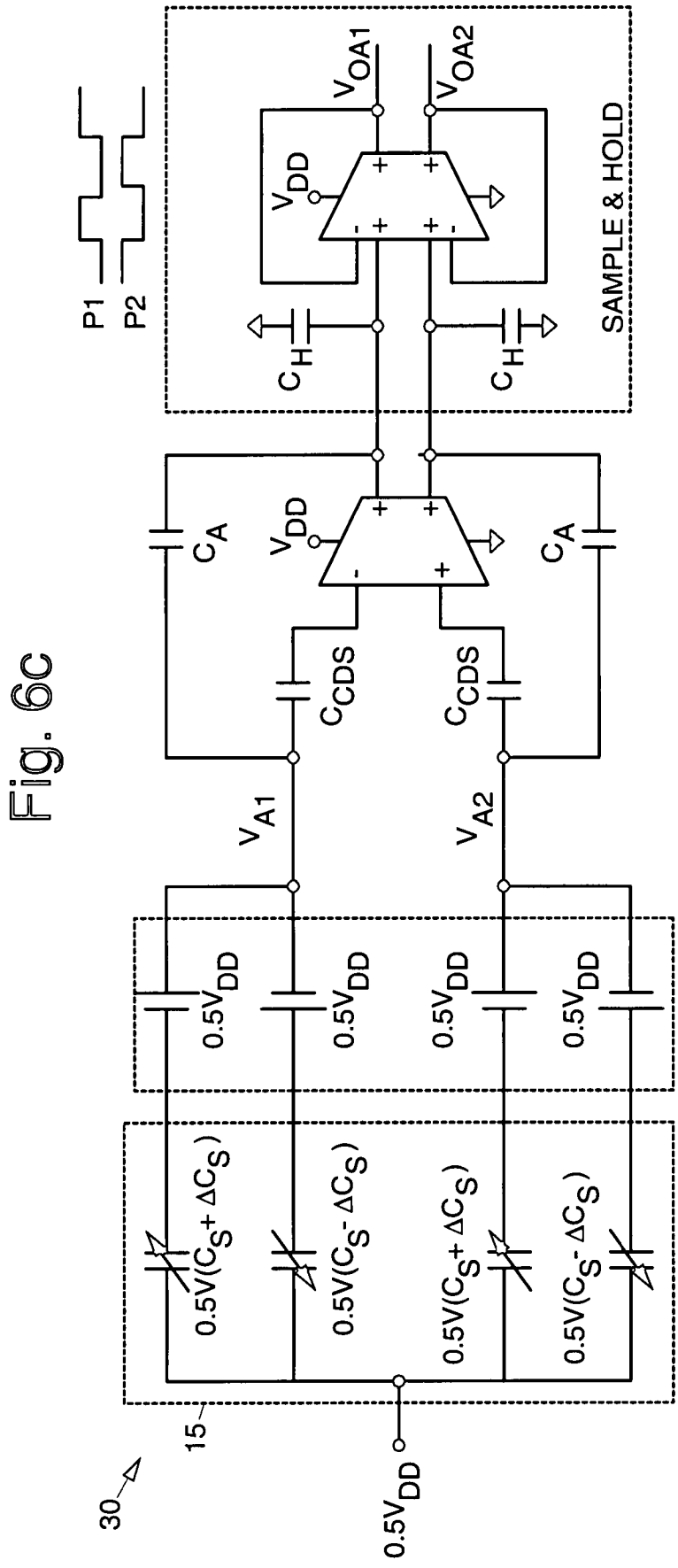
P1
P2
V_{OA1}
V_{OA2}
V_{DD}
C_H
C_H
SAMPLE & HOLD
C_A
V_{DD}
C_A
C_{CDS}
C_{CDS}
V_{A1}
V_{A2}
$0.5V_{DD}$
$0.5V_{DD}$
$0.5V_{DD}$
$0.5V_{DD}$
$0.5V(C_S+\Delta C_S)$
$0.5V(C_S-\Delta C_S)$
$0.5V(C_S+\Delta C_S)$
$0.5V(C_S-\Delta C_S)$
15
30
$0.5V_{DD}$

Fig. 6C

CAPACITIVE MICROACCELEROMETERS AND FABRICATION METHODS

STATEMENT REGARDING FEDERALLY SPONSORED RESEARCH OR DEVELOPMENT

This invention was made in part with government support under Grant Number NNC04GB18G awarded by National Aeronautics and Space Administration. Therefore, the government may have certain rights in this invention.

RELATED APPLICATIONS

This Application claims the benefit under 35 U.S.C. §120 of U.S. application Ser. No. 11/444,723, entitled "CAPACITIVE MICROACCELEROMETERS AND FABRICATION METHODS" filed on Jun. 1, 2006, which claims priority under 35 U.S.C. §119(e) to U.S. Provisional Application Serial No. 60/686,981, filed on Jun. 3, 2005, each of which is herein incorporated by reference in its entirety.

BACKGROUND

The present invention relates to microaccelerometers and methods for fabricating same.

Sub-micro-gravity accelerometers are used for measurement of very small vibratory disturbances on platforms installed on earth, space shuttles, and space stations as well as geophysical sensing and earthquake detection. However, the available systems are bulky, complex and expensive, and consume a lot of power. See, for example, Space Acceleration Measurement System (SAMS), http://microgravity.grc.nasa.gov/MSD/MSDhtmlslsamsff.html.

Due to the low-cost and high volume demand, the majority of commercially available microaccelerometers have been developed with low to medium range sensitivities. However, in the past few years, there has been an increasing demand for low-power and small form-factor micro-gravity (micro-g) accelerometers for a number of applications including vibration measurement and earthquake detection. High-performance digital microelectromechanical system (MEMS) accelerometers may also be utilized in ultra-small size for large-volume portable applications such as laptop computers, pocket PCs and cellular phones.

Despite the substantial improvements in micro-fabrication technology, which have enabled commercialization of low to medium sensitivity micromechanical accelerometers, the high precision (<10 μg resolution) accelerometer market has not been dominated by micromachined devices. Moreover, there has been an increasing demand for low-power and small footprint MEMS accelerometers with high sensitivity and stability for many applications such as oil exploration, gravity gradiometry, and earthquake detection. Inexpensive mass-production of these sensitive devices in small size not only can target all these existing applications but also could open new opportunities for applications never been explored with today's available bulky and complex measurement systems.

To achieve the overall device resolution in the sub-μg regime, both mechanical and electronic noises must be extensively suppressed. The dominant source of mechanical noise is the Brownian motion of air molecules hitting the circumferential surfaces of the small micromachined device. Increasing the inertial mass of the sensor is the most effective way of improving the device performance. One implementation of this approach using the full thickness of the silicon wafer combined with high aspect ratio sense gaps has been demonstrated and proved viable in realization of micro-gravity micromechanical accelerometers. Narrow sense gaps in these multiple-mask double-sided processes are defined by a sacrificial oxide layer, which is removed in a wet oxide-etch step referred to as a release step. Considering compliance of the structure required for high intended sensitivity, the sensitivity of the device is limited by the stiction in the wet release step.

The present inventors have previously disclosed 40 μm thick SOI accelerometers with 20 μg/√Hz resolution and sensitivity on the order of 0.2 pF/g. See B. Vakili Amini, S. Pourkamali, and F. Ayazi, "A high resolution, stictionless, CMOS-compatible SOI accelerometer with a low-noise, low-power, 0.25 μm CMOS interface," MEMS 2004, pp. 272-275. These accelerometers, however, do not have the structure or resolution capability of the present invention.

U.S. Pat. Nos. 6,287,885 and 6,694,814 disclose silicon-on-insulator devices designed as acceleration sensors. However, U.S. Pat. Nos. 6,287,885 and 6,694,814 do not disclose or suggest construction of an accelerometer having added seismic mass or the use of doped polysilicon to reduce capacitive gaps.

It would be desirable to have microaccelerometers that have improved submicron-gravity resolution.

BRIEF DESCRIPTION OF THE DRAWINGS

The various features and advantages of the present invention may be more readily understood with reference to the following detailed description taken in conjunction with the accompanying drawings, wherein like reference numerals designate like structural elements, and in which:

FIG. **1** is a schematic diagram of an exemplary differential capacitive SOI accelerometer;

FIG. **2** is a three-dimensional view of an exemplary differential capacitive SOI accelerometer;

FIGS. **3***a*-**3***d* are graphs showing design criteria for an exemplary accelerometer;

FIG. **3***e* is a graph showing Q variation with respect to gap size for an exemplary accelerometer;

FIGS. **4***a*-**4***c* illustrate an exemplary fabrication process flow for producing a differential capacitive SOI accelerometer;

FIGS. **4***d*-**4***f* illustrate an exemplary fabrication process flow for producing a differential capacitive silicon accelerometer;

FIG. **5***a* is a SEM picture of an exemplary accelerometer from the top side;

FIG. **5***b* is a SEM picture of an exemplary accelerometer from the bottom side showing extra proof mass;

FIG. **5***c* is a SEM picture of an exemplary accelerometer showing the proof mass, shock stop and comb drives;

FIG. **5***d* is a SEM picture showing sense electrodes with a reduced gap size;

FIG. **6***a* is a schematic diagram of an exemplary interface circuit for use with the accelerometer;

FIG. **6***b* is a diagram showing the exemplary interface circuit in a sampling phase; and

FIG. **6***c* is a diagram showing the exemplary interface circuit in an amplification phase.

DETAILED DESCRIPTION

Disclosed herein are micro- and submicro-gravity capacitive micro-machined accelerometers **10** (FIGS. **1** and **2**) interfaced to a low-power, low-noise reference-capacitor-less switched-capacitor interface circuit (FIG. **7***a*). The accelerometers **10** may be fabricated on relatively thick (>100 μm)

silicon-on-insulator (SOI) substrates **11** (FIGS. **3***a*-**3***c*) or on silicon substrates **11** (FIGS. **3***d*-**3***f*) using a high-aspect ratio fully-dry release process sequence that provide a large seismic mass and reduced in-plane stiffness. An SOI substrate is comprised of a silicon device layer, a buried oxide layer and a silicon handle layer. In the most general term, the silicon in the substrate can be replaced with other materials such as metals, including SiC and diamond. The resolution and sensitivity of fully-dry-released SOI accelerometers **10** are each improved by 100 times compare to earlier implementations to achieve, for the first time, deep sub-micro-gravity resolution in a small footprint (<0.5 cm^2).

FIG. **1** is a schematic diagram of an exemplary differential capacitive SOI accelerometer **10**. FIG. **2** is a three-dimensional view of an exemplary differential capacitive SOI accelerometer **10**.

The exemplary differential capacitive SOI accelerometer **10** comprises a silicon-on-insulator substrate **11** or wafer **11** comprising a lower silicon handle layer **12** and an upper silicon layer **13** (or device layer **13**) separated by an insulating layer **14**. The upper silicon layer **13** or device layer **13** is fabricated to comprise a proof mass **15** having a plurality of tethers **16** extending therefrom to an exterior portion of the upper silicon layer **13** or device layer **13** that is separated from the proof mass **15**. A portion of the insulating layer **14** and lower silicon handle layer **12** of the wafer **11** is attached to the proof mass **15** to provide added mass for the accelerometer **10**. The proof mass **15** also has a plurality of fingers **17** extending laterally therefrom. A plurality of electrodes **18** having readout fingers **19** extending therefrom are disposed adjacent to and separated from the plurality of fingers **17** extending from the proof mass **15**. Variable capacitors are formed between respective adjacent pairs of fingers **17**, **19** of the proof mass **15** and electrodes **18**. As is shown in FIG. **1**, a plurality of comb drive electrodes **21** having a plurality of fingers **22** to are interposed between comb drive fingers **23** extending from the proof mass **15**. The comb drive electrodes **21** are not shown in FIG. **2**.

One unique aspect of the present accelerometers **10** is the fact that it has added proof mass **15** comprising portion of the insulating layer **14** and lower silicon handle layer **12**. This provides for improved submicro-gravity resolution. Another unique aspect of the accelerometers **10** is that sense gaps between adjacent fingers **17**, **19** are very small, on the order of 9 μm.

Specifications for the accelerometer **10** are presented in Table 1. The accelerometer **10** has been designed to achieve the goal objectives for open loop operation in air.

TABLE 1

Specifications	
Static sensitivity	>5 pF/g
Brownian noise floor	<200 ng√Hz
Dynamic range	>100 dB
Frequency range	<200 Hz
Quality factor	<1
SOI thickness	>100 μm
Proof mass size	5 mm × 7 mm
Overall sensor size	7 mm × 7 mm
Mass	>10 milligram

The Brownian noise-equivalent acceleration (BNEA) may be expressed as

$$BNEA = \frac{\sqrt{4k_BTD}}{M} = \sqrt{\frac{4k_BT\omega_0}{MQ}} \propto \frac{1}{(capacitivegap)^{3/2}} \quad (1)$$

where K_B is the Boltzmann constant, T is the absolute temperature, ω_0 is the natural angular frequency (first flexural mode) of the accelerometer **10**, and Q is the mechanical quality factor. Increasing the mass and reducing the air damping improves this mechanical noise floor. However, reducing the damping increases the possibility of resonance (high-Q) and sensitivity to higher order modes, which is not desirable. Another limiting factor is the circuit noise equivalent acceleration (CNEA) that depends on the capacitive resolution of the interface IC (ΔC_{MIN}) and the capacitive sensitivity (S) of the accelerometer **10**:

$$CNEA = \frac{\Delta C_{\min}}{S}\left[\frac{\mathrm{m/s^2}}{\sqrt{\mathrm{Hz}}}\right] \quad (2)$$

The design objective is to minimize the Brownian noise equivalent acceleration (BNEA) and to maximize the static sensitivity (S) while satisfying process simplicity and size limitations. The exemplary fabrication process (FIGS. **3***a*-**3***c*) enables increase of the seismic mass **15** (to suppress the BNEA) and reduction of gap sizes (to increase S and reduce Q), independently. BNEA is a function of capacitive gap size and reduces for larger gaps (Equation 1). A deposited polysilicon layer **27** (or conformal conductive layer **27**) changes the thickness of the tethers **16** as well, which causes the mechanical compliance and therefore the sensitivity to start increasing for thinner polysilicon layers **27**.

FIGS. **3***a*-**3***d* are graphs showing design criteria for an exemplary accelerometer. FIG. **3***e* is a graph showing Q variation with respect to gap size for an exemplary accelerometer. A capacitive gap size between 4 and 8 μm satisfies the BNEA and S requirements for the accelerometer **10**. However, the Q for the accelerometer **10** should be in the overdamped region. Since the seismic mass **11** is relatively large (tens of milligrams) and the accelerometer **10** is very compliant, the accelerometer **10** may be vulnerable to damage caused by mechanical shock. Hence, shock stops and deflection limiters may be used to protect the accelerometer **10** and avoid nonlinear effects caused by momentum of the off-plane center of mass. ANSYS® simulation predicts the first mode shape (in-plane flexural) to occur at 180 Hz and the next mode shape (out-of-plane motion) to occur at 1300 Hz, which is well above the in-plane motion.

FIGS. **4***a*-**4***c* illustrate an exemplary two-mask fabrication process or method for fabricating exemplary SOI accelerometers **10**. The accelerometer fabrication process flow is as follows.

As is shown in FIG. **4***a*, a relatively thick silicon oxide layer **25** is deposited/grown on either one or both sides of a low resistivity relatively thick SOI wafer **11** (substrate **11**) comprising the silicon handle layer **12** and device layer **13**) separated by the insulating layer **14**. The oxide layer **25** is patterned on either one or both sides of the wafer **11** to form a deep reactive ion etching (DRIE) mask. The mask prevents further lithography steps after the device layer **13** is etched to define the structure of the accelerometer **10**. Trenches **26** (gaps **26**) are etched on the front side of the masked wafer **11** using the DRIE mask.

As is shown in FIG. **4***b*, a LPCVD polysilicon layer **27** is uniformly deposited on the SOI wafer **11** to reduce the size of the capacitive gaps **26** and doped to reduce the resistivity. A very thin conformal protection layer (such as LPCVD oxide) may be deposited to prevent the polysilicon on the sidewalls from getting attacked by etchant agents while etching back polysilicon in the next step. A blanket etch removes polysilicon at the bottom of the trenches **26** (capacitive gaps **26**) and provides isolation between pads **18** (electrodes **18**) and fingers **17**, **19**. In case the conformal protection layer is deposited, it should be removed from the surfaces before performing the polysilicon blanket etch step. For very high aspect ratio capacitive gaps **26**, the polysilicon at the bottom of the sense fingers cannot be removed from the top and consequently is etched from the back side. As is shown in FIG. **4***c*, the handle layer **12** is etched to expose the oxide buffer layer **14** from the back side of the wafer **12**. A portion of handle layer **12** on the back side of the proof mass **15** remains intact to add a substantial amount of mass to the accelerometer **10**.

The oxide buffer layer **14** is dry etched using an inductive plasma etching system, for example, and the accelerometer **10** is released. This fully-dry release process is a key to high-yield fabrication of extremely compliant structures with small capacitive gaps **26** without experiencing stiction problems caused by wet etching processes. The proof mass **15** is solid with no perforations to maximize sensitivity and minimize the mechanical noise floor per unit area. The residues of the oxide masking layer **25** are removed wherever the silicon is required to be exposed for electrical connection purposes.

An extra mask (not shown) may be used to reduce the height of the back-side seismic mass **15** (for packaging purposes). Also, the added mass of the proof mass **15** may be shaped to reduce the overall sensitivity of the accelerometer **10**. In addition, other compatible materials may be used instead of polysilicon **27** for the purpose of gap-reduction (e.g. polysilicon-germanium, for example). A separate mask may be added for top side trench etching to define the tethers **16** after deposition of the polysilicon layer **27**. In doing so, the width of the tethers **16** that determine the stiffness of the accelerometer **10** will not be affected by the deposited polysilicon layer **27**.

FIGS. **4***d*-**4***f* illustrate an exemplary fabrication process flow for fabricating exemplary silicon accelerometers **10**. The accelerometer fabrication process flow is as follows.

As is shown in FIG. **4***d*, a relatively thick oxide layer **25** is deposited/grown on either one or both sides of a low resistivity relatively thick silicon wafer **11** (silicon substrate **11**) and patterned (only the bottom oxide mask layer **25** is shown), and the top side is etched using deep reactive ion etching (DRIE), for example. The deep reactive ion etching produces trenches **26** (capacitive gaps **26**) adjacent the top surface of the silicon substrate **11**.

As is shown in FIG. **4***e*, a LPCVD polysilicon layer **27** is deposited on the silicon substrate **11** to reduce the size of the capacitive gaps **26**. The LPCVD polysilicon layer **27** is uniformly doped. A thin protection layer (such as LPCVD oxide) can be deposited to protect the sidewalls from being attacked while the polysilicon layer is etched from the back side in the consequent steps. This thin layer is etched back from the surfaces of the polysilicon (if deposited).

As is shown in FIG. **4***f*, a handle substrate **11***a* (e.g. glass or oxidized silicon) with interconnect through-holes is bonded to the top surface of the accelerometer. The cap substrate is previously patterned to carry shallow cavities above the movable parts of the structure. Electrical connections **29** to the electrodes is created through via holes in the substrate **11***a* and connect to the doped LPCVD polysilicon layer **27** on pads **18** formed in the lower substrate **11**. The silicon substrate **11** and the polysilicon deposited **27** at the bottom of the trenches is etched from the back side using deep reactive ion etching (DRIE) tools, for example, to release the accelerometer **10**. The etching leaves a portion of the bottom silicon substrate **11** as part of the proof mass **15**.

FIG. **5***a* is a SEM picture of an exemplary reduced-to-practice accelerometer **10** from the top side fabricated using the process described with reference to FIGS. **4***a*-**4***c*. FIG. **5***b* is a SEM picture of the reduced-to-practice accelerometer **10** from the bottom side showing extra proof mass **15**. FIG. **5***c* is a SEM picture of the reduced-to-practice accelerometer **10** showing the proof mass, shock stop and comb drives. FIG. **5***d* is a SEM picture showing sense electrodes of the reduced-to-practice accelerometer **10** with a reduced gap size.

The ability to control the amount of added mass is a powerful design parameter, which can be adjusted to achieve different sensitivities using the same top side device layout. Another important feature of the process flow discussed above is the gap reduction technique that utilizes conformal low pressure chemical vapor deposition (LPCVD) of polysilicon on the sidewalls of the trenches etched in the silicon. This fabrication method can also enable implementation of bi-axial and tri-axial accelerometers within a single embodiment.

The accelerometer **10** may be interfaced to a switched-capacitor charge amplifier integrated circuit (IC) **30** that eliminates the need for area-consuming reference capacitors. In this architecture, the reference capacitor is absorbed in the sense capacitance of the accelerometer **10** without compromising the sensitivity of the device or increasing area. The sense capacitance of the sensor is split into four identical sub-capacitances in a fully symmetric and differential manner (two increasing and two decreasing). The proof mass **11** is tied to a constant voltage source (half of the supply) at all times and is never clocked. This, in turn, simplifies the digital clock generator circuit and decreases the charge injection noise. By eliminating the need for reference capacitors and delayed version of the clock, our new interface architecture results in a significant reduction in the electronic die size. A correlated double sampling scheme may be used for strong suppression of the low-frequency flicker noise and offset. The interfacing is done through wire-bonds to the low noise and low power switched-capacitor IC implemented in a 2.5V 0.25 μm N-well CMOS. Alternatively, the interface circuit can be integrated with the accelerometer (or sensor) substrate on a common substrate to simplify packaging.

A schematic diagram of an exemplary accelerometer interface IC **30**, or circuit **30**, is shown in FIG. **6***a*. A switched-capacitor charge amplifier **31** eliminates the need for reference capacitors and has virtually zero input offset voltage. This is discussed by B. Vakili Amini, S. Pourkamali, M. Zaman, and F. Ayazi, in "A new input switching scheme for a capacitive micro-g accelerometer," Symposium on VLSI Circuits 2004, pp. 310-313. FIG. **6***b* is a diagram showing the exemplary interface circuit **30** in a sampling phase. FIG. **6***c* is a diagram showing the exemplary interface circuit **30** in an amplification phase.

Previously reported switched-capacitor charge amplifiers for capacitive sensors required on-chip reference capacitors to set the input common mode voltage. See, for example, B. Vakili Amini, and F. Ayazi, "A 2.5V 14-bit Sigma-Delta CMOS-SOI capacitive accelerometer," IEEE J. Solid-State Circuits, pp. 2467-2476, December 2004, W. Jiangfeng, , G. K. Fedder, and L. R. Carley, "A low-noise low-offset capacitive sensing amplifier for a 50-μg/√Hz monolithic CMOS MEMS accelerometer," IEEE I Solid-State Circuits, pp. 722-

730, May 2004, and H. Kulah, C. Junseok, N. Yazdi, and K. Najafi, "A multi-step electromechanical Sigma-Delta converter for micro-g capacitive accelerometers," ISSCC 2003, pp. 202-203. In the architecture disclosed herein, the reference capacitor is absorbed in the sense capacitance of the accelerometer **10** without compromising the sensitivity of the device or increasing area.

An exemplary interface IC **30** was fabricated using a 0.25 μm CMOS process operating from a single 2.5V supply and was wire-bonded to the accelerometer **10**. A low power consumption of 6 mW was observed. The effective die area is about 0.65 mm^2. In order to reduce the CNEA and improve the dynamic range, low frequency noise and offset reduction techniques, i.e., correlated double sampling and optimized transistor sizing were deployed. Moreover, the differential input-output scheme reduces the background common mode noise signals. The measured sensitivity is 83 mV/mg and the interface IC output noise floor is −91 dBm/Hz at 10 Hz, corresponding to an acceleration resolution of 170 ng/√Hz. The IC output saturates with less than 20 mg (less than 10 from earth surface). The interface IC **30** has a chip area of 0.5×1.3 mm^2. An exemplary fabricated IC **30** had a power consumption of 6 mW and core area of 0.65 mm^2.

The resolution and sensitivity of the fully-dry-released SOI accelerometers **10** are each improved by about 100 times to achieve, for the first time, deep sub-micro-gravity resolution in a small footprint (<0.5 cm^2). The figure-of-merit, defined as the ratio of device sensitivity to its mechanical noise floor, is improved by increasing the size of the solid seismic mass **11** by saving part of the handle layer **13** attached to the proof mass **11** (as shown in FIG. **2**). Also, capacitive gap sizes are reduced through deposition of the doped LPCVD polysilicon layer **16**, which relaxes the trench etching process and allows for higher aspect ratios.

As was mentioned above, the sense capacitance is split into four substantially identical sub-capacitances in a fully symmetric and differential manner. Thus, the reference capacitor is integrated into the sense capacitance of the accelerometer **10** and this does not compromise sensitivity or increase its area. The proof mass **11** is tied to a constant voltage source at all times and is never switched. By eliminating the need for reference capacitors, the interface architecture results in a generic front-end with significant reduction in the electronic die size. The front-end IC **30** may be implemented using a 2.5V 0.25 μm 2P5M N-well CMOS process, for example. Correlated double sampling scheme (CDS) is used for strong suppression of the low-frequency flicker noise and offset.

The following are unique features of fabricated microaccelerometers **10**. A two-mask process provides for high yield and a simple implementation. Fully-dry release provides for stictionless compliant devices. Gap size reduction provides for high capacitive sensitivity. Small aspect ratio trenches allow relaxed DRIE. Extra backside seismic mass provides for nano-gravity. No release perforation (solid proof mass) provides for maximum performance per unit area.

Thus, implementation and characterization of in-plane capacitive microaccelerometers **10** with sub-micro-gravity resolution and high sensitivity have been disclosed. The fabrication process produces stictionless accelerometers **10** and is very simple compared to conventional microaccelerometer fabrication techniques that use regular silicon substrates with multi-mask sets. These conventional techniques are discussed, for example, by P. Monajemi, and F. Ayazi, in "Thick single crystal Silicon MEMS with high aspect ratio vertical air-gaps," SPIE 2005 Micromachining/Microfabrication Process Technology, pp. 138-147, and J. Chae, H. Kulah, and K. Najafi., in "An in-plane high sensitivity, low-noise micro-g silicon accelerometer," MEMS 2003, pp. 466-469. The fully-dry release process provides for accelerometers **10** with maximum sensitivity and minimum mechanical noise floor per unit area. The accelerometers **10** may be interfaced with a generic sampled data front-end IC **30** that has the versatility of interfacing capacitive microaccelerometers **10** with different rest capacitors. Proper mechanical design keeps the accelerometers **10** in over-damped region in air that avoids unpredictable resonant response.

TABLE 2

Accelerometer and Interface IC Specifications

Accelerometer	
Top-side roof mass dimensions	7 mm × 5 mm × 120 μm
Extra seismic mass dimensions	5 mm × 3 mm × 400 μm
Proof mass	24 milli-gram
Sensitivity	17 pF/g
Brownian noise floor	100 nano-g/√Hz
f_{-3dB} (1^{st}-flexural)	180 Hz
2^{nd}-mode (out-of-plane)	1300 Hz
Gap size	5 μm
Interface IC	
Gain	83 mV/milli-g
Output noise floor	−91 dBm @ 10 Hz
Min. detectable Accl.	170 nano-g @ 10 Hz
Capacitive resolution	2 aF/√Hz @ 10 Hz
Power supply	GND-2.5 V
Power dissipation	6 mW
Sampling frequency	200 kHz
Die core area	0.65 mm^2

The sub-micro-gravity accelerometers **10** have applications in measurement of vibratory disturbances on the platforms installed on earth, space shuttles, and space stations, as well as in inertial navigation.

The use of thick SOI substrates in implementing lateral capacitive accelerometers has the advantage of increased mass compared to the polysilicon surface micromachined devices, which results in reduced Brownian noise floor for these devices. However, bulk silicon accelerometers are typically limited by the electronic noise floor, which can be improved by increasing the sensitivity (delta(C)/g) of the micromachined device. This usually requires an increase in the capacitive area and a reduction in the stiffness of the device, which in turn increases the possibility of stiction.

Thus, 120 μm-thick high sensitivity silicon capacitive accelerometers **10** on low-resistivity SOI substrates **11** using a backside dry-release process have been disclosed that eliminates stiction along with the need for perforating the proof mass **15**. A solid proof mass **15** with no perforations results in a smaller footprint for the sensor and an improved electromechanical design. An improved architecture interface circuit **30** is also disclosed that has no limitation of sensing large capacitive (>10 pF) microaccelerometers **10**.

Thus, microaccelerometers and fabrication methods relating thereto have been disclosed. It is to be understood that the above-described embodiments are merely illustrative of some of the many specific embodiments that represent applications of the principles discussed above. Clearly, numerous and other arrangements can be readily devised by those skilled in the art without departing from the scope of the invention.

What is claimed is:

1. A method of fabricating a moveable microstructure, comprising:

providing a substrate having upper and lower layers;

etching trenches in the upper layer to define bonding pads, sense electrodes and a proof mass having capacitive

gaps formed therebetween, and a plurality of tethers that allow the proof mass to move;

depositing a conformal conductive layer on the substrate to reduce sizes of the capacitive gaps;

etching the conformal conductive layer to remove conformal conductive material at the bottom of the trenches and provide isolation between the bonding pads and the sense electrodes; and

etching the lower layer of the substrate to form a region of extra proof mass that is coupled to the proof mass formed in the upper layer.

2. The method recited in claim **1** wherein the conformal conductive layer is doped to reduce its electrical resistance.

3. The method recited in claim **1** further comprising:

masking and etching the back side of the proof mass to reduce its height.

4. The method recited in claim **1** wherein the substrate comprises a silicon-on-insulator substrate.

5. The method recited in claim **1** wherein the substrate comprises a silicon substrate.

6. A method of fabricating a moveable microstructure, comprising:

providing a low resistivity silicon-on-insulator substrate;

etching wenches on the front side of the substrate to define bonding pads, sense electrodes and a proof mass having capacitive gaps formed therebetween;

depositing a conformal conductive layer on the substrate to reduce capacitive gap sizes;

doping the conformal conductive layer;

etching the conformal conductive layer to remove material at the bottom of the trenches; and

etching the back side of the substrate to form a region of additional proof mass and to release the microstructure.

7. The method recited in claim **6** further comprising:

growing a thermal silicon oxide layer on both sides of the substrate;

patterning the oxide layer on the both sides of the substrate to form an etch mask.

8. A method of fabricating a moveable microstructure, comprising:

providing a silicon substrate;

etching trenches on the front side of the substrate to define pads, sense electrodes and a proof mass having capacitive gaps formed therebetween;

depositing a conformal conductive layer on the substrate to reduce capacitive gap sizes;

bonding a handle substrate to the top side of the silicon substrate;

etching the back side of the substrate to form a region of additional proof mass and to release the microstructure by etching the conformal conductive layer to remove material at the bottom of the trenches; and

forming electrical connections through via holes in the handle substrate to the conformal conductive layer adjacent to pads defined in the silicon substrate.

9. The method recited in claim **8** wherein the bonded handle substrate comprises an oxidized silicon substrate.

* * * * *

UNITED STATES PATENT AND TRADEMARK OFFICE

CERTIFICATE OF CORRECTION

PATENT NO. : 7,757,393 B2
APPLICATION NO. : 11/904804
DATED : July 20, 2010
INVENTOR(S) : Farrokh Ayazi et al.

It is certified that error appears in the above-identified patent and that said Letters Patent is hereby corrected as shown below:

At column 9, claim 6, line 24, please change "etching wenches" to -- etching trenches --.

Signed and Sealed this

Fifth Day of October, 2010

David J. Kappos

David J. Kappos
Director of the United States Patent and Trademark Office

UNITED STATES PATENT AND TRADEMARK OFFICE

CERTIFICATE OF CORRECTION

PATENT NO. : 7,757,393 B2
APPLICATION NO. : 11/904804
DATED : July 20, 2010
INVENTOR(S) : Farrokh Ayazi, Babak Vakili Amini and Reza Abdolvand

It is certified that error appears in the above-identified patent and that said Letters Patent is hereby corrected as shown below:

On the Title Page insert item (62)

--Related U.S. Application Data
(62) Division of application No. 11/444,723, filed on June 1, 2006, now Pat. No. 7,337,671, which claims benefit of Provisional application No. 60/686,981, filed on June 3, 2005--

Signed and Sealed this
First Day of March, 2011

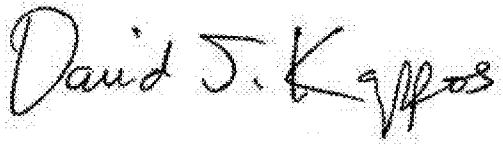

David J. Kappos
Director of the United States Patent and Trademark Office